PAPER

A graphitic-C$_3$N$_4$ derivative containing heptazines merged with phenyls: synthesis, purification and application as a high-efficiency metal-free quasi-green phosphor for white LEDs†

Huaijun Tang, [ID] *[a] Qiuhong Chen,[a] Guoyun Meng,*[b] Shiyou Lu,[a] Jing Qin,[a] Kaixin Yang,[a] Long Gao,[a] Zhengliang Wang [ID] [a] and Yonghui He*[c]

Because rare-earth elements are scarce, expensive, and unsustainable, it is of great significance to develop rare-earth-free (even metal-free) luminescent materials as phosphors for LEDs. Here, a graphitic-C$_3$N$_4$ (g-C$_3$N$_4$) derivative containing some heptazines merged with phenyls has been synthesized *via* thermal polymerization of melamine and quinazoline-2,4(1*H*,3*H*)-dione at an optimal mole ratio of 18 : 1. In comparison with g-C$_3$N$_4$ synthesized from melamine only, the photoluminescent (PL) emission colour changed from blue to green, the maximum emission wavelength ($\lambda_{em,max}$) changed from 467 nm to 508 nm, and the PL quantum yield (PLQY) increased from 8.0% to 24.0%. It was further purified *via* vacuum sublimation, and a product with yellowish green emission ($\lambda_{em,max}$ = 517 nm) and PLQY up to 45.5% was obtained. This sublimated product had high thermal stability and low thermal quenching; its thermal decomposition temperature was as high as 527 °C, and its relative PL emission intensity at 100 °C was 90.8% of that at 20 °C. Excited by blue light chips ($\lambda_{em,max}$ ≈ 460 nm), cold, neutral and warm white LEDs can be fabricated using the sublimated product and orange-emitting (Sr,Ba)$_3$SiO$_5$:Eu^{2+} as phosphors. The good performances of these white LEDs (for example, the CIE coordinates, color rendering index and correlated color temperature were (0.31, 0.33), 84.4 and 6577 K, respectively) suggest that the low-efficiency blue-emitting g-C$_3$N$_4$ had been successfully converted into a high-efficiency metal-free quasi-green phosphor.

1. Introduction

Carbon nitride (C$_3$N$_4$) is one of the oldest artificial polymers and can be traced back to 1834.[1-5] However, it hardly attracted any attention until it was predicted as a new superhard material in 1989.[6] To date, five different phases of C$_3$N$_4$ have been reported, including α-C$_3$N$_4$, β-C$_3$N$_4$, cubic-C$_3$N$_4$, pseudocubic-C$_3$N$_4$ and graphitic-C$_3$N$_4$ (g-C$_3$N$_4$).[1-5,7] Among them, the first four types are mainly used as superhard materials;[6-9] the last type (*i.e.*, g-C$_3$N$_4$) consists of robust two-dimensional (2D) layered

polymers, which is the most stable phase of C$_3$N$_4$ at ambient conditions.[1-5] Now, g-C$_3$N$_4$ and its derivatives/composites have widely attracted interdisciplinary attention due to their outstanding advantages, such as high stability, strong photo-responsivity and photoelectric conversion capability, facile synthesis, low cost, earth-abundance, non-toxicity, and environment-friendliness.[1-5] They have been widely applied in catalysis (especially, as metal-free photocatalysts),[1-4,10] energy conversion and storage,[5,11] separation membranes,[12] luminescent materials,[13-19] and other fields.

Mainly due to the radiative transition between the π, σ (or δ) antibonding orbitals (related to sp^2 C–N bond) and the lone pair (LP) in the 2p orbitals of the edge N (*i.e.*, π* → LP and σ* → LP), g-C$_3$N$_4$ can emit blue light (mainly at 430–550 nm with the maximum wavelength at around 470 nm).[1,13-19] When it is properly modified (such as covalent atomic/molecular doping),[20-25] light of other longer wavelength colours also can be achieved; therefore, g-C$_3$N$_4$ and its derivatives can be used as luminescent materials in some fields, such as light-emitting diodes (LEDs),[14,20-23,26] luminescence detection[16,17] and bio-imaging.[17-19,22,24] It is known that g-C$_3$N$_4$ includes two allotropes with the basic structural units of coplanar tri-*s*-triazine (*i.e.*,

aKey Laboratory of Green-Chemistry Materials in University of Yunnan Province, National and Local Joint Engineering Research Center for Green Preparation Technology of Biobased Materials, School of Chemistry & Environment, Yunnan Minzu University, Kunming, 650500, P. R. China. E-mail: tanghuaijun@sohu.com

bDepartment of Chemistry, Key Lab of Organic Optoelectronics and Molecular Engineering of Ministry of Education, Tsinghua University, Beijing, 100084, P. R. China. E-mail: mengguoyun@sina.com

cKey Laboratory of Chemistry in Ethnic Medicinal Resources, State Ethnic Affairs Commission & Ministry of Education, Yunnan Minzu University, Kunming 650500, China. E-mail: hee_csu@126.com

† Electronic supplementary information (ESI) available: Some figures and data of sample preparation, characterizations, and luminescent properties. See DOI: https://doi.org/10.1039/d3ra00473b

heptazine, C_6N_7) and triazine (C_3N_3), respectively.[1–5] Relatively, heptazine-based g-C_3N_4 is more stable[2–5] and has better luminescence properties due to its bigger π-conjugated system and higher electron delocalization.[27,28]

It is well-known that LEDs are gradually replacing traditional light sources (such as incandescent lamps and fluorescent lamps) and are widely applied in general lighting, displays, automotive headlamps, visible light communication and so on, due to their advantages including high efficiency, energy-saving nature, long life, and environmental protection.[29–32] LEDs (especially, the most important white LEDs) usually are fabricated using ultraviolet-/blue-light-emitting chips and down-conversion luminescent materials (*i.e.*, phosphors).[29–32] All kinds of luminescent materials have been tried as phosphors in LEDs in the past; however, up to now, the successfully commercialized phosphors almost are rare-earth-based inorganic luminescent materials (such as $Y_3Al_5O_{12}:Ce^{3+}$ and La_2-$Ce_2O_7:Eu^{3+}$)[31,32] mainly due to their high luminous efficiency and good heat resistance. However, rare-earth elements are very expensive and scarce; their mining and refining are accompanied by heavy pollution and high energy consumption, which are unsustainable in the long run. Therefore, developing phosphors without rare-earth elements is very significant and necessary, and hence has become a new research hotspot.[33,34] At present, rare-earth-free phosphors mainly include some organic materials, inorganic quantum dots (QDs), perovskites, and Mn^{4+}-doped fluorides.[33,34]

g-C_3N_4-based phosphors also are rare-earth-free (actually, metal-free) and have some other outstanding advantages for LEDs. For example, they can be easily prepared *via* thermal polymerization from cheap and source-abundant precursors, including melamine, cyanamide, monocyanamide, urea, thiourea, dicyandiamide, guanidinium chloride and so on.[1–5] Due to the thermal polymerization process, they usually are highly stable up to *ca.* 600 °C even in the air,[1–5] which is enough to meet the thermal requirements for LEDs since their fabrication and working processes usually are below 150 °C. Nevertheless, pristine bulk g-C_3N_4 is difficult to be used in LEDs because it just emits blue light with low efficiency, and its solid-state quantum yield (QY) usually is around 5%.[15,23] Tuning the emission light colour from blue to the longer wavelength region and improving the luminous efficiency at the same time are two key requirements for g-C_3N_4-based luminescent materials to be successfully applied in LEDs and other fields. Some strategies, including atomic/molecular doping,[20–25] nanosizing (including quantum dots),[15–19,26,35] composite fabrication,[15] and heterojunction construction[36] have been used to achieve the above purposes. For example, in 2019, a series of g-C_3N_4 derivatives emitting multiple colours (450–650 nm) were synthesized using urea (as the precursor) and 2-aminothiophene-3-carbonitrile (as the dopant) by Q. Guo *et al.*;[20] then, high-quality white LEDs were prepared using these g-C_3N_4 derivatives as the phosphors. In 2020, by using 2,4-diamino-6-phenyl-1,3,5-triazine as the precursor, phenyl-modified g-C_3N_4 with a broad emission range (500–650 nm) and high QY (about 60%) was synthesized by S. Porcu *et al.*,[21] and a white LED was successfully fabricated by using it as a phosphor together with a blue light chip. Right this,

phenyl-modified and sulfur-atom-doped g-C_3N_4-based nanomaterials with longer wavelength emission were prepared and used in white LEDs by H. Zhang *et al.*[22] Recently, we prepared naphthyl-modified g-C_3N_4 by using melamine and cyanuric acid as precursors and 6-(naphthalen-2-yl)-1,3,5-triazine-2,4-diamine as the dopant; relative to bulk g-C_3N_4, the emission of this product was in the longer wavelength region, along with a wider spectrum and higher QY, and it was also successfully used in white LEDs.[23] Despite such encouraging progress, g-C_3N_4-based luminescent materials used in LEDs (especially, white LEDs) are still very rare and unsatisfactory. Some disadvantages, such as uncontrollable emission colour, low luminous efficiency, and poor batch stability need to be overcome urgently for their wide application.

For g-C_3N_4-based luminescent materials, molecular doping is an effective way to improve the luminous efficiency and tune emission colour;[20–25] however, the luminous efficiency usually decreases when too much of organic dopants are used,[20,22,23] probably due to too many structural defects, oversized π-conjugated systems, very low energy gaps and some undesired impurities,[3,4] which result in high charge separation and luminescence quenching. Therefore, the amount of organic dopant used needs to be optimized. Additionally, the luminous efficiency can be further improved if some over-polymerized components with oversized π-conjugated systems and undesired impurities are separated (*i.e.*, purification). Based on these viewpoints, here, a yellowish-green-emitting g-C_3N_4 derivative containing some heptazines merged phenyls was synthesized by using melamine and quinazoline-2,4(1H,3H)-dione at an optimal mole ratio and further purified by vacuum sublimation. Then, the sublimated product (*i.e.*, purified product) was successfully used as a high-efficiency metal-free quasi-green phosphor in white LEDs under the excitation of GaN-based blue light chips.

2. Experimental details

2.1 General information

Melamine (AR, Adamas-Beta, Shanghai, China), quinazoline-2,4(1H,3H)-dione (AR, Alfachem Co., Ltd, Zhengzhou, China), $(Sr,Ba)_3SiO_5:Eu^{2+}$ (Looking Long Technology Co., Ltd, Shenzhen, China) and epoxy resin (Guangyihe Glue Co., Ltd, Shenzhen, China) were used without further purification. The g-C_3N_4-based luminescent materials were purified by using a vacuum-sublimation purifier (BOF-2-50, AnHui BEQ Equipment Technology CO., Ltd, Hefei, China). Powder X-ray diffraction (PXRD) measurements were made by using a Bruker AXS D8 Advance A25 Powder X-ray Diffractometer (Bruker, Switzerland) with a graphite-monochromatized Cu Kα radiation (λ = 1.5406 Å, 40 kV and 30 mA). The ^{13}C Solid-state NMR spectra were obtained on a Bruker AVANCE III 400 M spectrometer (Bruker, Switzerland). The scanning electron micrographs were obtained using an FEI Nova NanoSEM450 scanning electron microscope (FEI, U.S.A.). The IR spectra were measured with KBr pellets on a Nicolet iS10 FT-IR spectrometer (Thermo Fisher, U.S.A.). The ultraviolet-visible-near infrared diffuse reflectance spectra (UV-Vis-NIR DRS) were measured on a Hitachi U-4100

spectrophotometer (Hitachi, Japan). The PL spectra, PL decay curves, and quantum yield at room temperature were measured on an FLS920 fluorescence spectrophotometer (Edinburgh, U. K.). The temperature-dependent PL spectra were measured on a Cary Eclipse FL1011M003 spectrofluorometer (Varian, U.S.A.) with a temperature controller (REX-C110, Kaituo Compressor Parts Co. Ltd, Dongguan, China). Thermogravimetry (TG) was performed on a Netzsch STA449F3 thermal analyzer (NETZSCH, Germany) at a heating rate of 10 °C min^{-1} under N_2 flow.

2.2 Synthesis of g-C$_3$N$_4$ and its derivatives

g-C$_3$N$_4$ was synthesized *via* thermal polymerization (at 500 °C) by using only melamine as the precursor. A series of g-C$_3$N$_4$ derivatives containing some heptazines merged with phenyls (g-C$_3$N$_4$-Ph) were also synthesized *via* thermal polymerization (at 500 °C, as shown in Scheme 1) from melamine and quinazoline-2,4(1*H*,3*H*)-dione at different molar ratios of $x:1$ ($x = 12, 14, 16, 18, 20, 22$ and 24, respectively). The detailed synthetic process was as follows. Melamine and quinazoline-2,4(1*H*,3*H*)-dione were ground in an agate mortar for about 0.5 h; the resulting fine powders were placed into a corundum crucible, which then was wrapped by a piece of aluminium foil. After making several small holes in the aluminium foil on the top of the crucible using a syringe needle, the crucible was heated in an Ar atmosphere to 500 °C at a heating rate of 2.5 °C min^{-1} and maintained for 2 h. After being cooled to room temperature, the pale-yellow solid product was obtained, with a yield of around 65.0%.

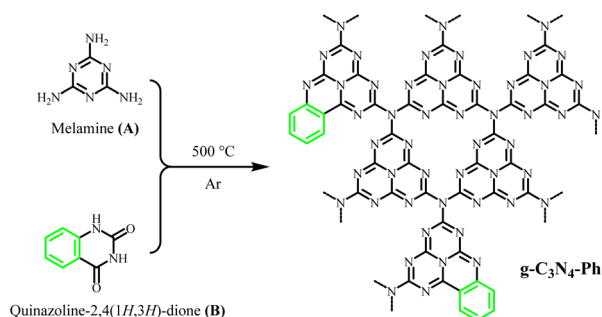## 2.3 Fabrication and performance measurements of LEDs

For LED fabrication, the phosphors (g-C$_3$N$_4$-Ph and (Sr,Ba)$_3$-SiO$_5$:Eu^{2+}) were blended in the epoxy resin matrix at certain weight percentages (wt%); the mixtures were stirred homogeneously and coated on blue-emitting chips ($\lambda_{em,max} \approx 460$ nm) until the reflective cavities just were filled up. The LEDs were placed in a vacuum drying oven, dried at 80 °C for 1 h and solidified at 110 °C for 2 h. The LEDs were operated at 5 V forward voltage and 20 mA forward current. The emission spectra of the LEDs were recorded on a high-accuracy array spectrometer (HSP6000), and their performance data were measured using an integrating sphere spectroradiometer

system (PMS-50) (Everfine Optoelectronics Technology Co. Ltd, Hangzhou, China).

3. Results and discussion

3.1 Synthesis and purification

As shown in Scheme 1, a series of g-C$_3$N$_4$-Ph was synthesized by employing melamine and quinazoline-2,4(1*H*,3*H*)-dione at different molar ratios. For luminescent materials, their photoluminescent (PL) emission intensity is an important and key parameter, so it was used as the parameter for optimizing the molar ratio in this work. All of them emitted green light mainly in the 455–600 nm range with the maximum wavelengths ($\lambda_{em,max}$) at around 508 nm (Fig. 1). From 24 : 1 to 12 : 1, the amount of quinazoline-2,4(1*H*,3*H*)-dione was increased successively, and the PL emission intensity of the corresponding products first increased, reached the maximum at 18 : 1, and then decreased successively. Therefore, 18 : 1 was chosen as the optimal molar ratio. This product was further used in subsequent studies, and g-C$_3$N$_4$-Ph represents the product prepared at this molar ratio unless otherwise stated. This g-C$_3$N$_4$-Ph was further purified *via* vacuum sublimation ($\leq 4.0 \times 10^{-6}$ mbar, 420 °C), the sublimated part was collected as the final product (s-g-C$_3$N$_4$-Ph), a yellow solid (Fig. S1†) with a yield of 28.8%. However, the sublimation of g-C$_3$N$_4$ was not successfully achieved by us, especially under the same sublimation conditions used for g-C$_3$N$_4$-Ph. We think that part of g-C$_3$N$_4$-Ph sublimated successfully mainly due to the phenyl rings at the edge. These phenyl rings without –NH$_2$ cannot further link to other heptazines (as shown in Scheme 1), which would prevent the expansion of the 2D polymeric sheets and result in relatively small-sized 2D sheets with low molecular weight. On the contrary, the 2D sheets in g-C$_3$N$_4$ can expand to very large sizes, so g-C$_3$N$_4$ could not be sublimated successfully.
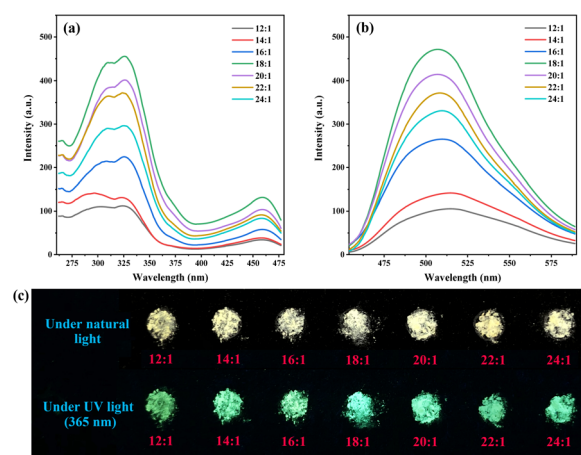

Fig. 1 (a) The PL excitation and (b) emission spectra, and (c) photographs of g-C$_3$N$_4$-Ph synthesized using melamine and quinazoline-2,4(1*H*,3*H*)-dione at molar ratios 12 : 1, 14 : 1, 16 : 1, 18 : 1, 20 : 1, 22 : 1 and 24 : 1, respectively. $\lambda_{ex} = 326$ nm, $\lambda_{em} = 508$ nm.

Scheme 1 The synthesis of g-C$_3$N$_4$-Ph. Molar ratios $A:B = x:1$ ($x = 12, 14, 16, 18, 20, 22$, and 24).
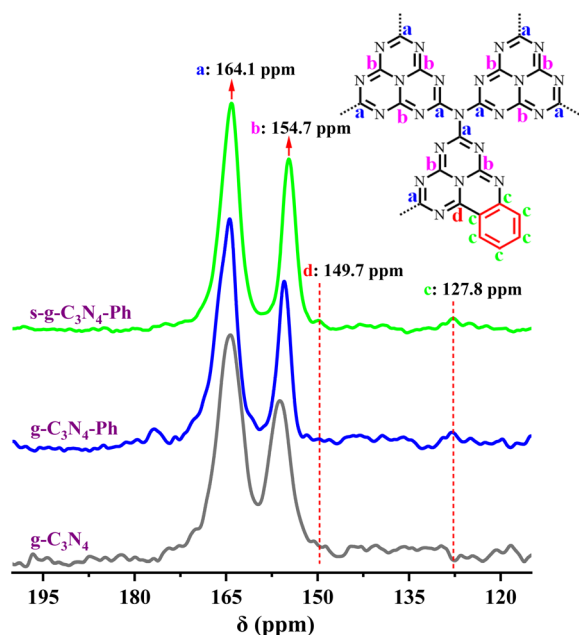
Fig. 2 The solid-state ^{13}C NMR spectra of g-C_3N_4, g-C_3N_4-Ph and s-g-C_3N_4-Ph. (Inset) The representative structural units of g-C_3N_4-Ph and s-g-C_3N_4-Ph.

3.2 Characterization

The ^{13}C solid-state NMR (^{13}C SSNMR) spectrum of g-C_3N_4 (Fig. 2) showed two strong signal peaks (164.3 ppm and 156.2 ppm), which can be ascribed to the C atoms (No. a and b in Fig. 2) in the heptazine units.[37,38] Similarly, two strong peaks also appeared on the spectra of g-C_3N_4-Ph (164.4 ppm and 155.5 ppm) and s-g-C_3N_4-Ph (164.1 ppm and 154.7 ppm), which indicates that all of them were mainly made up of heptazines. However, there were two other weak peaks at around 127.8 ppm and 149.7 ppm on their spectra but not on that of g-C_3N_4; the peak at around 127.8 ppm originated from the C atoms (no. c in Fig. 2) in the phenyl rings, and the other peaks around 149.7 ppm were very weak but visible and could be attributed to the C atoms (No. d in Fig. 2) near the phenyl rings.
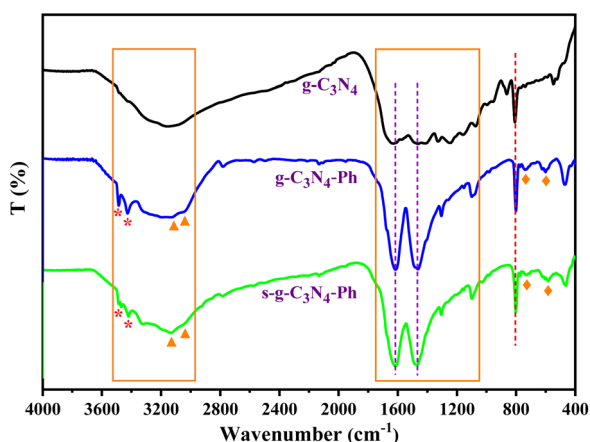
The FT-IR spectra of g-C_3N_4, g-C_3N_4-Ph and s-g-C_3N_4-Ph (Fig. 3) showed the typical breathing vibration of heptazines at around 805 cm^{-1} (orange dashed line in Fig. 3) and the stretching modes of C–N/C=N of heptazines at 1050–1750 cm^{-1},[22–24] which also indicate that all of them were mainly made up of heptazines. Due to the overlap of the skeleton vibration absorption of the phenyl rings with the stretching vibration absorption region of C–N/C=N, in the g-C_3N_4-Ph and s-g-C_3N_4-Ph spectra, this absorption region became stronger and sharper (1465 cm^{-1} and 1615 cm^{-1}, purple dashed lines in Fig. 3). Moreover, the stretching vibration absorption (3040 cm^{-1} and 3125 cm^{-1}, orange triangles in Fig. 3) and out-of-plane wagging vibration absorption (740 cm^{-1} and 595 cm^{-1}, orange rhombuses in Fig. 3) of C–H further suggested that the phenyls had merged with some heptazines. On all three spectra, the broad absorption band at 3000–3500 cm^{-1} could be ascribed to the N–H stretching vibration of the uncondensed amine groups (mainly at the edges of the 2D sheets).[20,22,23] However, although some heptazines are merged via phenyls in g-C_3N_4-Ph and s-g-C_3N_4-Ph, because these units cannot link to other heptazines due to the absence of amino groups on the phenyls, the 2D sheets become relatively small-sized, and the proportion of amine groups at the edges relatively increases; thus, the stretching vibration absorption of N–H (3485 cm^{-1} and 3425 cm^{-1}, orange stars in Fig. 3) became stronger.

The XRD pattern of g-C_3N_4 (Fig. 4) was completely consistent with those reported in the literature,[10,13,37] showing low crystallinity and only two distinct diffraction peaks, of which the strong peak at 27.2° indexed to (002) diffraction originates from the interplanar graphitic stacking, while the weak peak at 13.1° corresponding to (100) diffraction belongs to the in-plane structural packing of the heptazines. However, there were some sharp peaks on the XRD patterns of g-C_3N_4-Ph and s-g-C_3N_4-Ph, nearly the same as those of melem oligomers with a low polymerization degree,[39] which suggests that g-C_3N_4-Ph and s-g-C_3N_4-Ph also had low polymerization degrees and were composed of small-sized 2D sheets. These small-sized 2D sheets are easier to crystallize than the large-sized g-C_3N_4 2D sheets, so g-C_3N_4-Ph and s-g-C_3N_4-Ph had higher crystallinity than g-C_3N_4.

The scanning electron microscopic (SEM) images of g-C_3N_4, g-C_3N_4-Ph and s-g-C_3N_4-Ph (Fig. 5) are in good agreement with

Fig. 3 The FT-IR spectra of g-C_3N_4, g-C_3N_4-Ph and s-g-C_3N_4-Ph.
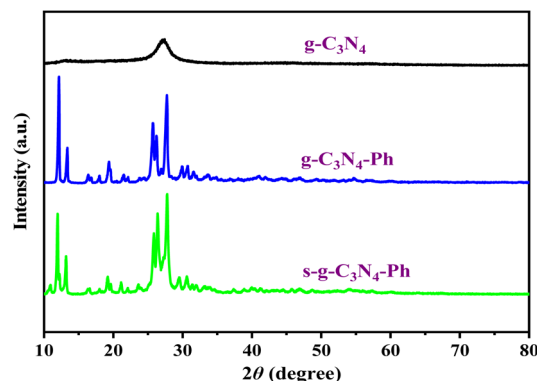
Fig. 4 Powder XRD patterns of g-C_3N_4, g-C_3N_4-Ph and s-g-C_3N_4-Ph.
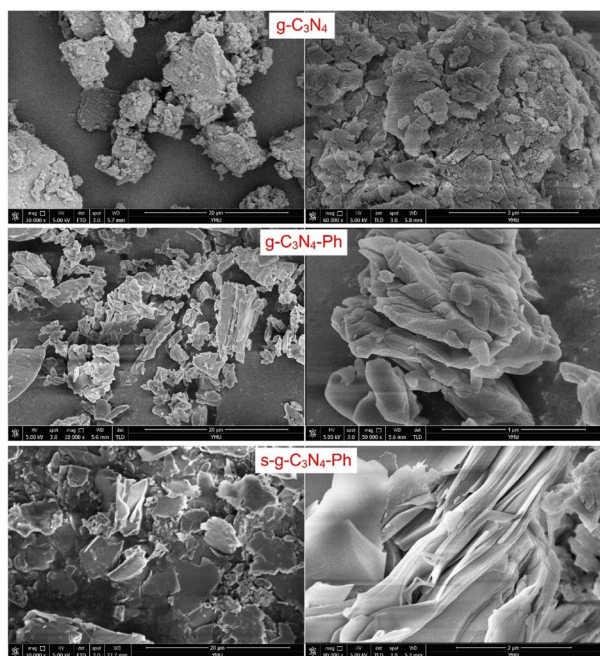
Fig. 5 The SEM images of g-C$_3$N$_4$, g-C$_3$N$_4$-Ph and s-g-C$_3$N$_4$-Ph.

the results of their XRD. All of them were composed of stacked sheets; however, the stack of g-C$_3$N$_4$ was very messy (corresponding to its low crystallinity), while the other two were relatively more regular and compact (corresponding to their higher crystallinity). Especially, some s-g-C$_3$N$_4$-Ph slices composed of many single 2D sheets could be clearly identified.

The ultraviolet-visible-near infrared diffuse reflectance spectra (UV-Vis-NIR DRS) and the corresponding Tauc plots (Fig. 6) showed that the absorbance threshold of the g-C$_3$N$_4$ powders was about 450 nm, and the corresponding optical band gap energy (E_g) was about 2.76 eV, which are consistent with those in the literature.[10,37] The absorption of g-C$_3$N$_4$-Ph and s-g-C$_3$N$_4$-Ph showed an obvious red-shift relative to that of g-C$_3$N$_4$ due to the merging of some heptazines with phenyls and the resultant extension of their π-conjugated systems; their absorbance thresholds were about 719 nm and 539 nm, and the E_g were 2.30 eV and 1.72 eV, respectively. Because the relatively big-

sized 2D sheets with bigger π-conjugated systems were separated after vacuum sublimation, the absorption of s-g-C$_3$N$_4$-Ph showed an obvious blue shift (180 nm) relative to that of g-C$_3$N$_4$-Ph, and its E_g correspondingly increased from 1.72 eV to 2.30 eV.

The above characterization results (^{13}C NMR, FT-IR, XRD, SEM and UV-Vis-NIR DRS) indicate the merging of the phenyl rings from quinazoline-2,4(1H,3H)-dione with heptazines; in other words, the expected target products (g-C$_3$N$_4$-Ph and s-g-C$_3$N$_4$-Ph) were obtained. Furthermore, the chemical structure of the sublimated product (s-g-C$_3$N$_4$-Ph) was basically consistent with that of the product before sublimation (g-C$_3$N$_4$-Ph), but the 2D sheets with a high polymerization degree and high molecular weights no longer existed in s-g-C$_3$N$_4$-Ph.

3.3 The PL properties of g-C$_3$N$_4$, g-C$_3$N$_4$-Ph and s-g-C$_3$N$_4$-Ph

The intrinsic PL emission of g-C$_3$N$_4$ (without modification) is blue light,[14,15,23] in this work, it also emitted blue light mainly at 425–575 nm with the $\lambda_{em,max}$ of 467 nm (Fig. 7). The PL emission of g-C$_3$N$_4$-Ph showed an obvious red shift (41 nm) relative to that of g-C$_3$N$_4$ and was in the green light region (455–625 nm, $\lambda_{em,max}$ = 508 nm) mainly because the phenyl rings had merged with some heptazines. Moreover, one N atom of every such heptazine is replaced by one C atom with lower electronegativity (as shown in Scheme 1), which results in the enhanced delocalization of the π-conjugated system and narrowing of the bandgap, thereby enhancing the PL emission efficiency and intensity at the same time.[5,20–25] The increase of heptazines merging with phenyls was beneficial to improving PL emission, so the PL emission intensity of g-C$_3$N$_4$-Ph enhanced with the increasing amount of quinazoline-2,4(1H,3H)-dione but reached the maximum at 18 : 1 molar ratio of melamine and quinazoline-2,4(1H,3H)-dione (Fig. 1) and then decreased sharply probably because of the quick increase in structural defects and impurities (such as the potential self-polymerization products of quinazoline-2,4(1H,3H)-dione). Relative to the 8.0% QY of g-C$_3$N$_4$, the QY of g-C$_3$N$_4$-Ph (at 18 : 1) had significantly improved to 24.0%.
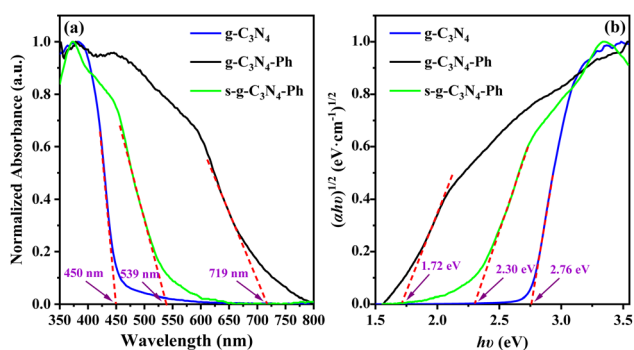
Fig. 6 (a) The UV−Vis−NIR DRS and (b) the corresponding Tauc plots of g-C$_3$N$_4$, g-C$_3$N$_4$-Ph and s-g-C$_3$N$_4$-Ph.
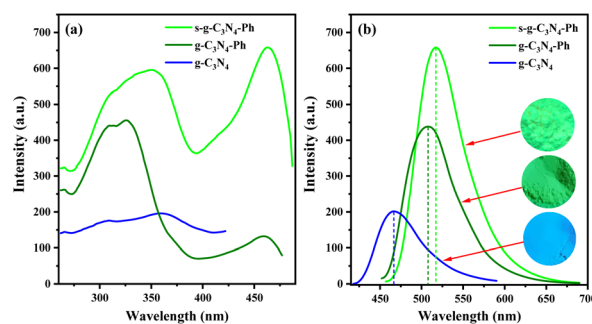
Fig. 7 (a) The PL excitation and (b) emission spectra of g-C$_3$N$_4$ (λ_{ex} = 361 nm, λ_{em} = 467 nm), g-C$_3$N$_4$-Ph (λ_{ex} = 326 nm, λ_{em} = 508 nm) and s-g-C$_3$N$_4$-Ph (λ_{ex} = 463 nm, λ_{em} = 517 nm). (Inset) From bottom to top, photographs of g-C$_3$N$_4$, g-C$_3$N$_4$-Ph and s-g-C$_3$N$_4$-Ph under a 365 nm UV lamp.

The sublimated product s-g-C_3N_4-Ph emitted a bright yellowish-green light (460–650 nm, $\lambda_{em,max}$ = 517 nm). Relative to the PL emissions of g-C_3N_4 ($\lambda_{em,max}$ = 467 nm) and g-C_3N_4-Ph ($\lambda_{em,max}$ = 508 nm), that of s-g-C_3N_4-Ph showed a red-shift of 50 nm and 9 nm, respectively. This also can be attributed to the merging of heptazines with phenyls. As mentioned above, the degree of polymerization and size of the 2D sheets of s-g-C_3N_4-Ph were lower than those of g-C_3N_4-Ph; moreover, the purity of s-g-C_3N_4-Ph was higher than that of g-C_3N_4-Ph. Therefore, it is reasonable to believe that the 2D sheets in s-g-C_3N_4-Ph are more closely packed together than those in g-C_3N_4-Ph (as shown in Fig. 5), which causes a higher degree of π–π stacking and results in the red-shift of PL emission (9 nm). Due to the big-sized 2D sheets with low luminous efficiency and the separation of some undesired impurities, the QY of s-g-C_3N_4-Ph greatly improved and reached 45.5% which is much higher than those of g-C_3N_4 (8.0%) and g-C_3N_4-Ph (24.0%). As far as we know, s-g-C_3N_4-Ph is the first high-efficiency g-C_3N_4-based luminescent product obtained by using vacuum sublimation as the purification technique.

As shown in Fig. 7, the excitation spectra of g-C_3N_4-Ph and s-g-C_3N_4-Ph were very different from that of g-C_3N_4; especially, they had a relative red-shift in excitation (at around 460 nm), which also can mainly be due to the effect of phenyl ring modification. Both g-C_3N_4-Ph and s-g-C_3N_4-Ph showed two peaks on their excitation spectra; both left peaks were mainly at 272–395 nm, and the $\lambda_{ex,max}$ of the left peaks of g-C_3N_4-Ph and s-g-C_3N_4-Ph were 326 nm and 361 nm, respectively. Their right peaks were similar to each other, mainly at 395–480 nm with the $\lambda_{ex,max}$ of 459 nm and 463 nm, respectively. These peaks should have mainly originated from the units of heptazine merging with phenyl. Relative to the right peak of g-C_3N_4-Ph, that of s-g-C_3N_4-Ph was much stronger perhaps due to the higher proportion of heptazine merging with phenyls and the high purity of s-g-C_3N_4-Ph. At the same time, the right peak of s-g-C_3N_4-Ph was stronger than its left peak, which means that s-g-C_3N_4-Ph can be efficiently excited by blue light and hence can be used together with commercial GaN-based blue light chips. The PL data of g-C_3N_4, g-C_3N_4-Ph and s-g-C_3N_4-Ph are further summarized in Table S1.† In view of the better PL emission performance of s-g-C_3N_4-Ph, only it was further studied and used in LEDs.

3.4 The optical and thermal properties of s-g-C_3N_4-Ph

The solid-state PL decay of s-g-C_3N_4-Ph at room temperature was triexponential with an average lifetime of 38 ns (Fig. S3†); such nanosecond-level lifetime suggests that it has potential application in general lighting, displays, etc.[13]

As shown in Fig. 8, the thermogravimetry (TG) curve suggested that s-g-C_3N_4-Ph has very high thermal stability; its thermal decomposition temperature (T_d) was as high as 527 °C, which is high enough to meet the heat-resistance requirements for LEDs (>150 °C).[23,40] The thermal quenching property of s-g-C_3N_4-Ph was investigated by its temperature-dependent PL spectra measured at every 20 °C interval from 20 °C to 200 °C (Fig. 9); the results are summarized in Table S2.† When the
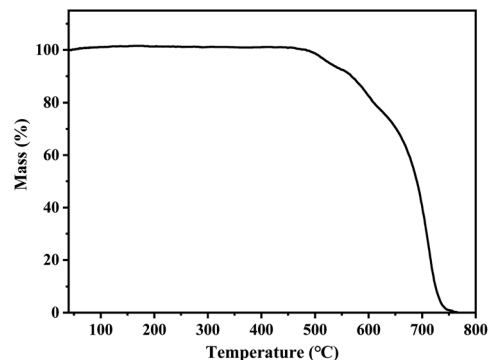

Fig. 8 The TG curve of s-g-C_3N_4-Ph.

temperature was increased from 20 °C to 200 °C, the PL emission range and spectra shape hardly changed, except for a slight red-shift of $\lambda_{em,max}$ (from 517 nm to 520 nm), which suggests that its emission color is very stable and hardly changes with the increase of temperature. At the same time, the decline of its emission intensity was not serious with the rising temperature, and its relative emission intensity at 100 °C was 90.8% of that at 20 °C, the relative intensity at 160 °C (10 °C higher than 150 °C, as required for LEDs) was 82.0% of that at 20 °C, and even at 200 °C, 77.2% intensity was retained. Thermal quenching was very low and lower than those of many inorganic phosphors,[40,41] so s-g-C_3N_4-Ph is a good candidate phosphor for LEDs.

3.5 Application of s-g-C_3N_4-Ph in LEDs

Under the excitation of GaN-based blue light chips ($\lambda_{em,max} \approx$ 460 nm), when only s-g-C_3N_4-Ph blended in epoxy resin was used as the phosphor, the blue light of the chips was completely absorbed at the blending concentration of 8.0 wt% (Fig. 10(a)), and a yellowish-green LED (No. a) with emission only from s-g-C_3N_4-Ph was obtained; its CIE coordinates were (0.30, 0.56), $\lambda_{em,max}$ was 517 nm, and the luminous efficiency was 20.7 lm W^{-1} (Table 1).
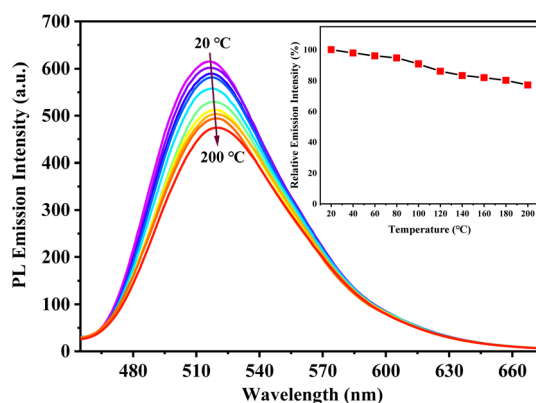

Fig. 9 The temperature-dependent PL spectra (λ_{ex} = 463 nm) of the s-g-C_3N_4-Ph powder measured at every 20 °C interval from 20 °C to 200 °C. (Inset) The relative PL emission intensity at the $\lambda_{em,max}$ of the s-g-C_3N_4-Ph powder as a function of temperature.
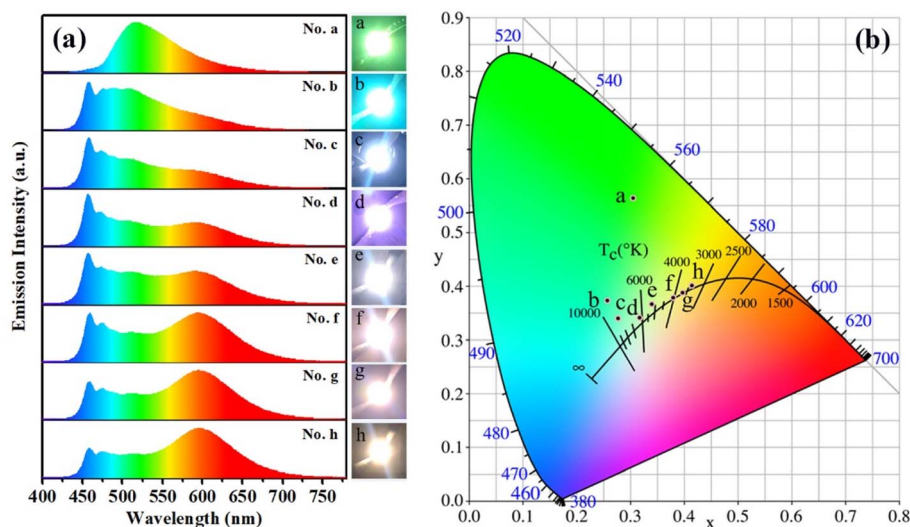
Fig. 10 (a) The emission spectra of LEDs No. a–h. Insets on the right: photographs of the LEDs in the working state. (b) The CIE coordinates of LEDs No. a–h.

Further, s-g-C$_3$N$_4$-Ph was used for fabricating white LEDs together with commercial orange phosphors (Sr,Ba)$_3$SiO$_5$:Eu^{2+} ($\lambda_{em,max}$ = 598 nm)[42] and excited by the above blue light chips. As listed in Table 1, the blending concentration of s-g-C$_3$N$_4$-Ph in every LED was fixed at 3.0 wt%, the blending concentration of (Sr,Ba)$_3$SiO$_5$:Eu^{2+} was changed from 0.50 wt% to 2.00 wt%. The emission spectra of all these LEDs (No. b–h) are shown in Fig. 10(a). The spectra were composed of three components, including the blue light of the chips, the green light of s-g-C$_3$N$_4$-Ph and the red light of (Sr,Ba)$_3$SiO$_5$:Eu^{2+}. With increasing concentration of (Sr,Ba)$_3$SiO$_5$:Eu^{2+}, the blue light gradually was absorbed and faded; at the same time, the red light gradually enhanced, and relatively, the proportion of the green light of s-g-C$_3$N$_4$-Ph in every LED was more stable. Except for LED No. b, the other LEDs (No. c–h) were white, and their correlate colour temperatures (CCT) gradually decreased from 8426 K to 3374 K with increasing concentrations of (Sr,Ba)$_3$SiO$_5$:Eu^{2+}. Among them, No. c (CCT = 8426 K) and No. d (CCT = 6577 K) were cold white LEDs, No. e (CCT = 5250 K) and No. f (CCT = 4027 K) were neutral white LEDs, and No. g (CCT = 3647 K) and No. h (CCT =

3374 K) were warm white LEDs. Such continuous change in their emission colour is exhibited by their CIE coordinates and working state photographs (Fig. 10). The white LEDs showed high colour rendering indexes (CRI); except for No. c (CRI = 77.5), the CRI of other white LEDs were higher than 80. At the same time, all of them showed high luminous efficiencies, mostly between 50.0 lm W^{-1} and 60.0 lm W^{-1}. Taken together, the white LEDs emitted high-quality white light; especially, LEDs No. d and No. e possessed high CRI (84.4 and 83.8, respectively), and their CIE coordinates (0.31, 0.33) and (0.34, 0.37) were very close to those (0.33, 0.33) of pure white light. Though s-g-C$_3$N$_4$-Ph is a yellowish-green-emitting material, the results of its application in white LEDs suggest that it can provide a high-quality green light component for white light. Most of the reported green phosphors usually use rare-earth ions for green emission or sensitization, such as Ce$_5$Si$_3$O$_{12}$-N:Tb^{3+},[43] Ba$_2$LiSi$_7$AlN$_{12}$:Eu^{2+},[44] RbLi(Li$_3$SiO$_4$)$_2$:Eu^{2+},[45] CaY$_2$-HfGa(AlO$_4$)$_3$:Ce^{3+},[46] and CaY$_2$ZrScAl$_3$O$_{12}$:Ce^{3+}.[47] In comparison, s-g-C$_3$N$_4$-Ph is not only rare-earth-free but also metal-free, which makes it a cheap quasi-green phosphor for LEDs. Moreover, it

Table 1 The performance data of the LEDs[a]

| No. of LEDs | Blending concentration (wt%) | | Luminous efficiency (lm W^{-1}) | CRI | CCT (K) | $\lambda_{em,max}$ (nm) | CIE (x, y) |
	s-g-C$_3$N$_4$-Ph	(Sr,Ba)$_3$SiO$_5$:Eu^{2+}					
a	8.0	0.0	20.7	35.1	6024	517	(0.30, 0.56)
b	3.0	0.50	33.5	64.1	8847	457	(0.26, 0.37)
c	3.0	0.75	44.5	77.5	8426	458	(0.27, 0.34)
d	3.0	1.00	56.0	84.4	6577	457, 591	(0.31, 0.33)
e	3.0	1.25	50.4	83.8	5250	458, 593	(0.34, 0.37)
f	3.0	1.50	54.7	82.0	4027	459, 595	(0.38, 0.38)
g	3.0	1.75	60.0	81.5	3647	458, 594	(0.40, 0.39)
h	3.0	2.00	54.5	80.2	3374	459, 596	(0.41, 0.40)

[a] All LEDs were excited by GaN-based blue light chips, and their luminous efficiencies were around 25.0 lm W^{-1}, $\lambda_{em,max} \approx$ 460 nm. The CIE coordinates were around (0.15, 0.04), CCT > 100 000 K. All LEDs were operated at 5.0 V forward voltage and 20 mA forward current.

can be efficiently excited by GaN-based blue light chips, which are cheap now due to large-scale commercial production. Therefore, s-g-C$_3$N$_4$-Ph is a good phosphor for practical applications.

4. Conclusions

In summary, a g-C$_3$N$_4$ derivative was successfully synthesized *via* thermal polymerization using melamine and quinazoline-2,4(1*H*,3*H*)-dione at an optimal mole ratio of 18 : 1 and further purified *via* vacuum sublimation. Relative to unmodified pristine g-C$_3$N$_4$, the PL emission colour of sublimated product s-g-C$_3$N$_4$-Ph changed from blue ($\lambda_{em,max} = 467$ nm) to yellowish-green ($\lambda_{em,max} = 517$ nm); the QY significantly increased from 8.0% to 45.5%. Moreover, s-g-C$_3$N$_4$-Ph had high thermal stability and low thermal quenching. When excited by GaN-based blue light chips, cold, neutral and warm white LEDs could be fabricated by using this material as the green phosphor together with (Sr,Ba)$_3$SiO$_5$:Eu^{2+} as the orange phosphor. The good performances of the white LEDs suggest that s-g-C$_3$N$_4$-Ph is a promising high-efficiency metal-free quasi-green phosphor candidate.

Author contributions

Huaijun Tang: conceptualization, methodology, investigation, data curation, writing-original draft, writing-reviewing and editing, supervision, project administration, funding acquisition. Qiuhong Chen: conceptualization, methodology, investigation, data curation, writing-original draft. Guoyun Meng: conceptualization, methodology, investigation, data curation, supervision, project administration, resources. Shiyou Lu: investigation, data curation. Jing Qin: investigation, data curation. Kaixin Yang: investigation, data curation. Long Gao: investigation, data curation. Zhengliang Wang: methodology, resources, supervision. Yonghui He: methodology, investigation, data curation, writing-reviewing and editing.

Conflicts of interest

There are no conflicts to declare.

Acknowledgements

References

1 Y. Wang, X. Wang and M. Antonietti, *Angew. Chem., Int. Ed.*, 2012, **51**, 68–89.
2 D. Zhang, W. He, J. Ye, X. Gao, D. Wang and J. Song, *Small*, 2021, **17**, 2005149.
3 W.-J. Ong, L.-L. Tan, Y. H. Ng, S.-T. Yong and S.-P. Chai, *Chem. Rev.*, 2016, **116**, 7159–7329.
4 D. K. Chauhan, S. Jain, V. R. Battula and K. Kailasam, *Carbon*, 2019, **152**, 40–58.
5 Y. Luo, Y. Yan, S. Zheng, H. Xue and H. Pang, *J. Mater. Chem. A*, 2019, **7**, 901–924.
6 A. Y. Liu and M. L. Cohen, *Science*, 1989, **245**, 841–842.
7 D. M. Teter and R. J. Hemley, *Science*, 1996, **271**, 53–55.
8 C.-M. Sung and M. Sung, *Mater. Chem. Phys.*, 1996, **43**, 1–8.
9 Q. Wei, Q. Zhang, H. Yan and M. Zhang, *Materials*, 2016, **9**, 840.
10 X. Wang, K. Maeda, A. Thomas, K. Takanabe, G. Xin, J. M. Carlsson, K. Domen and M. Antonietti, *Nat. Mater.*, 2009, **8**, 76–80.
11 M. Ghaemmaghami and R. Mohammadi, *Sustainable Energy Fuels*, 2019, **3**, 2176–2204.
12 Y. Wang, B. Gao, Q. Yue and Z. Wang, *J. Mater. Chem. A*, 2020, **8**, 19133–19155.
13 Y. Zhang, Q. Pan, G. Chai, M. Liang, G. Dong, Q. Zhang and J. Qiu, *Sci. Rep.*, 2013, **3**, 1943.
14 J. Liu, H. Wang and M. Antonietti, *Chem. Soc. Rev.*, 2016, **45**, 2308–2326.
15 W. Liu, S. Xu, S. Guan, R. Liang, M. Wei, D. G. Evans and X. Duan, *Adv. Mater.*, 2018, **30**, 1704376.
16 S. Zhang, J. Li, M. Zeng, J. Xu, X. Wang and W. Hu, *Nanoscale*, 2014, **6**, 4157–4162.
17 Y.-C. Lu, J. Chen, A.-J. Wang, N. Bao, J.-J. Feng, W. Wang and L. Shao, *J. Mater. Chem. C*, 2015, **3**, 73–78.
18 X. Zhang, H. Wang, H. Wang, Q. Zhang, J. Xie, Y. Tian, J. Wang and Y. Xie, *Adv. Mater.*, 2014, **26**, 4438–4443.
19 M. Yang, H. Mei, Y. Shen, K. Wu, D. Pan, S. Liu, T. Zhang and Y. Zhang, *Chem.–Eur. J.*, 2019, **25**, 10188–10196.
20 Q. Guo, M. Wei, Z. Zheng, X. Huang, X. Song, S.-B. Qiu, X.-b. Yang, X. Liu, J. Qiu and G. Dong, *Adv. Opt. Mater.*, 2019, **7**, 1900775.
21 S. Porcu, I. Roppolo, M. Salaun, G. Sarais, S. Barbarossa, M. F. Casula, C. M. Carbonaro and P. C. Ricci, *Appl. Surf. Sci.*, 2020, **504**, 144330.
22 H. Zhang, D. Zheng, Z. Cai, Z. Song, Y. Xu, R. Chen, C. Lin and L. Guo, *ACS Appl. Nano Mater.*, 2020, **3**, 6798–6805.
23 H. Tang, Q. Chen, S. Lu, X. Li, H. Li, Y. Wang, K. Wang, Q. Zhou and Z. Wang, *J. Lumin.*, 2022, **244**, 118734.
24 Q. Cui, J. Xu, X. Wang, L. Li, M. Antonietti and M. Shalom, *Angew. Chem., Int. Ed.*, 2016, **55**, 3672–3676.
25 Z. Song, Z. Li, L. Lin, Y. Zhang, T. Lin, L. Chen, Z. Cai, S. Lin, L. Guo, F. Fu and X. Wang, *Nanoscale*, 2017, **9**, 17737–17742.
26 L. He, M. Fei, J. Chen, Y. Tian, Y. Jiang, Y. Huang, K. Xu, J. Hu, Z. Zhao, Q. Zhang, H. Ni and L. Chen, *Mater. Today*, 2019, **22**, 76–84.
27 J. Li, L. Tao, Y. Wang, Y. Yao and Q. Guo, *Front. Chem.*, 2021, **9**, 717569.
28 P. Audebert, E. Kroke, C. Posern and S.-H. Lee, *Chem. Rev.*, 2021, **121**, 2515–2544.
29 J. Y. Tsao, M. H. Crawford, M. E. Coltrin, A. J. Fischer, D. D. Koleske, G. S. Subramania, G. T. Wang, J. J. Wierer and R. F. Karlicek Jr, *Adv. Opt. Mater.*, 2014, **2**, 809–836.
30 J. Cho, J. H. Park, J. K. Kim and E. F. Schubert, *Laser Photonics Rev.*, 2017, **11**, 1600147.
31 S. Ye, F. Xiao, Y. X. PAN, Y. Y. Ma and Q. Y. Zhang, *Mater. Sci. Eng., R*, 2010, **71**, 1–34.

32 A. G. Bispo Jr, L. F. Saraiva, S. A. M. Lima, A. M. Pires and M. R. Davolos, *J. Lumin.*, 2021, **237**, 118167.

33 H. Zhang, H. Zhang, A. Pan, B. Yang, L. He and Y. Wu, *Adv. Mater. Technol.*, 2020, **6**, 2000648.

34 K. K. Thejas, M. Abraham, A. K. Kunti, M. Tchernycheva, S. Ahmad and S. Das, *Appl. Mater. Today*, 2021, **24**, 101094.

35 J. Zhou, Y. Yang and C.-Y. Zhang, *Chem. Commun.*, 2013, **49**, 8605–8607.

36 S. Bayan, N. Gogurla, A. Midya and S. K. Ray, *Carbon*, 2016, **108**, 335–342.

37 Z. Chen, P. Sun, B. Fan, Q. Liu, Z. Zhang and X. Fang, *Appl. Catal., B*, 2015, **170–171**, 10–16.

38 B. V. Lotsch, M. Döblinger, J. Sehnert, L. Seyfarth, J. Senker, O. Oeckler and W. Schnick, *Chem.–Eur. J.*, 2007, **13**, 4969–4980.

39 V. W. Lau, M. B. Mesch, V. Duppel, V. Blum, J. Senker and B. V. Lotsch, *J. Am. Chem. Soc.*, 2015, **137**, 1064–1072.

40 A. A. Setlur, R. J. Lyons, J. E. Murphy, N. P. Kumar and M. S. Kishore, *ECS J. Solid State Sci. Technol.*, 2013, **2**(2), R3059–R3070.

41 L. Chen, C. C. Lin, C. W. Yeh and R. S. Liu, *Materials*, 2010, **3**, 2172–2195.

42 L. Chen, A. Luo, Y. Jiang, F. Liu, X. Deng, S. Xue, X. Chen and Y. Zhang, *Mater. Lett.*, 2013, **106**, 428–431.

43 D. Wu, J. Zhou, X. Lin, J. Lin, L. Shi, J. Ding and Q. Wu, *ACS Appl. Electron. Mater.*, 2021, **3**, 406–414.

44 T. Takeda, N. Hirosaki, S. Funahshi and R.-J. Xie, *Chem. Mater.*, 2015, **27**, 5892–5898.

45 M. Zhao, H. Liao, L. Ning, Q. Zhang, Q. Liu and Z. Xia, *Adv. Mater.*, 2018, **30**, 1802489.

46 J. Chan, L. Cao, W. Li, N. Ma, Z. Xu and X. Huang, *Inorg. Chem.*, 2022, **61**, 6953–6963.

47 L. Cao, W. Li, B. Devakumar, N. Ma, X. Huang and A. F. Lee, *ACS Appl. Mater. Interfaces*, 2022, **14**, 5643–5652.